

# ACCRETING X-RAY PULSARS OBSERVED WITH *INTEGRAL*

Ingo Kreykenbohm<sup>1,2</sup>, Sonja Fritz<sup>1</sup>, Nami Mowlavi<sup>2</sup>, Jörn Wilms<sup>3</sup>, Peter Kretschmar<sup>4</sup>, Rüdiger Staubert<sup>1</sup>, and Andrea Santangelo<sup>1</sup>

<sup>1</sup>*Institut für Astronomie und Astrophysik – Abt. Astronomie, Sand 1, 72076 Tübingen, Germany*

<sup>2</sup>*Integral Science Data Centre, Chemin d’Ecogia 16, 1290 Versoix, Switzerland*

<sup>3</sup>*Dr. Remeis Sternwarte, Universität Erlangen-Nürnberg, Sternwartstr. 7, 96049 Bamberg, Germany*

<sup>4</sup>*European Space Astronomy Centre (ESA), Madrid, Spain*

## ABSTRACT

In this paper, we review the observational properties of two accreting X-ray pulsars, the persistent source 4U 1907+09 and the transient V 0332+53. Accreting X-ray pulsars are among the brightest sources in the X-ray sky and are frequently observed by *Integral* and other X-ray missions. Nevertheless they are still very enigmatic sources as fundamental questions on the X-ray production mechanism still remain largely unanswered. These questions are addressed by performing detailed temporal and spectral studies on several objects over a long time range.

Of vital importance is the study of cyclotron lines as they provide the only direct link to the magnetic field of the pulsar. While some objects show cyclotron lines which are extremely stable with time and with pulse phase, in other objects the lines strongly depend on the pulse phase, the luminosity of the source, or both.

Of special interest in any case are transient sources where it is possible to study the evolution of the cyclotron line and the source in general from the onset until the end of the outburst through a wide range of different luminosity states.

We present an observational review of a transient and a persistent accreting X-ray pulsar observed with *Integral*.

Key words: X-rays: stars – stars: magnetic fields – stars: flare – stars: pulsars: individual: 4U 1907+09 – stars: pulsars: individual: V0332+53 .

## 1. INTRODUCTION

Accreting X-ray pulsars are among the most prominent sources in the X-ray sky. Since accreting X-ray pulsars are usually young objects, they are clustered along the galactic plane. Although already discovered in the first days of X-ray astronomy, many fundamental questions remain unanswered to date. The X-ray production

mechanism is only roughly understood, as a detailed understanding would require a full magneto-hydrodynamic treatment, incorporating the presence of a magnetic field of  $\sim 10^{12}$  G, and a full handling of general relativity. Especially the behavior and shape of cyclotron resonant scattering features (CRSFs or cyclotron lines) are not very well understood and require detailed studying. But also only a very general picture of the overall accretion geometry and the accretion process itself exists. Analyzing the temporal behavior of accreting neutron stars along with the spectral properties allows to study these important questions.

*INTEGRAL* is an excellent instrument to study these sources as *INTEGRAL* frequently observes the galactic center and the galactic plane and due to its large field of view. As a result, an enormous amount of data on accreting X-ray pulsars is obtained. In this paper we present some recent results on the analysis of two accreting X-ray pulsars: the detection of a complete torque reversal in 4U 1907+09 [9] and the evolution of the transient V 0332+53 over its recent outburst and especially the behavior of the cyclotron line [27, 33].

## 2. 4U 1907+09

The wind-accreting High Mass X-ray Binary system 4U 1907+09 [13] consists of a neutron star in an eccentric ( $e = 0.28$ ) 8.3753 d orbit around its companion. Based on a lower limit for the distance of 5 kpc, the X-ray luminosity is approximately  $2 \cdot 10^{36}$  erg s<sup>-1</sup> [15]. The stellar companion has been classified as a O8–O9 Ia supergiant with an effective temperature of 30500 K, a radius of  $26 R_{\odot}$ , a luminosity of  $5 \cdot 10^5 L_{\odot}$ , and a mass loss rate of  $7 \cdot 10^{-6} M_{\odot}$  yr<sup>-1</sup> [6].

Similar to other accreting neutron stars, the X-ray continuum of 4U 1907+09 can be described by a power-law spectrum with an exponential turnover at  $\sim 13$  keV [25]. The spectrum is modified by strong photoelectric absorption with a column  $N_H = 1.5\text{--}5.7 \cdot 10^{22}$  cm<sup>-2</sup> [7] which is due to the dense stellar wind and is therefore strongly variable over the orbit. The column density is maximal

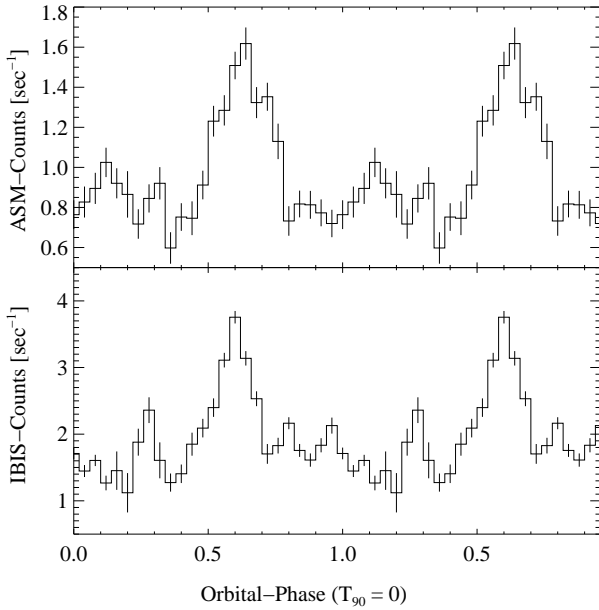


Figure 1. Light curve of 4U 1907+09, folded with the orbital period of 8.3753 days [from 9]. Upper Panel: Rossi X-ray Timing Explorer All Sky Monitor (ASM) 2–12 keV. Lower Panel: IBIS 20–40 keV light curve.

between the end of the primary X-ray flare and the start of the secondary flare (Fig. 1) of the orbital light curve [31]. At higher energies, the spectrum exhibits cyclotron resonant scattering features (CRSF) at  $\sim 19$  keV and  $\sim 40$  keV [24, 25, 7].

With a pulse period of  $\sim 440$  s, 4U 1907+09 is a slowly rotating neutron star [23]. The neutron star has exhibited a steady linear spin down with an average of  $\dot{P}_{\text{pulse}} = +0.225 \text{ s yr}^{-1}$  from  $P_{\text{pulse}} = 437.5$  s in 1983 to 440.76 s in 1998 [16]. Recently, a decrease in  $\dot{P}_{\text{pulse}}$  to  $\sim 0.115 \text{ s yr}^{-1}$ , about half the long term value was reported [2].

## 2.1. Timing Analysis

The X-ray light curve of 4U 1907+09 clearly shows pulsations with a period of  $\sim 441$  s. Additionally, 4U 1907+09 also exhibits flares with a typical length of several hours [23, 16]. Fritz et al. [9] observed four such flares with count rate increases of at least  $5\sigma$  over its normal level (Fig. 2). Three of them, in revolutions 187, 193, and 305, are associated with the main peak in the orbital light curve (Fig. 1) while the flare observed in revolution 188 is linked to the secondary peak.

4U 1907+09 showed a steady spin down rate of  $\dot{P}_{\text{pulse}} = +0.225 \text{ s yr}^{-1}$  [16]. Baykal et al. [2] using *RXTE*-data determined a spin down rate 0.5 times lower than the long term value. Fritz et al. [9] using *INTEGRAL* data, extend the tracking of the pulse period evolution to the years 2003–2005. Therefore these authors first determine

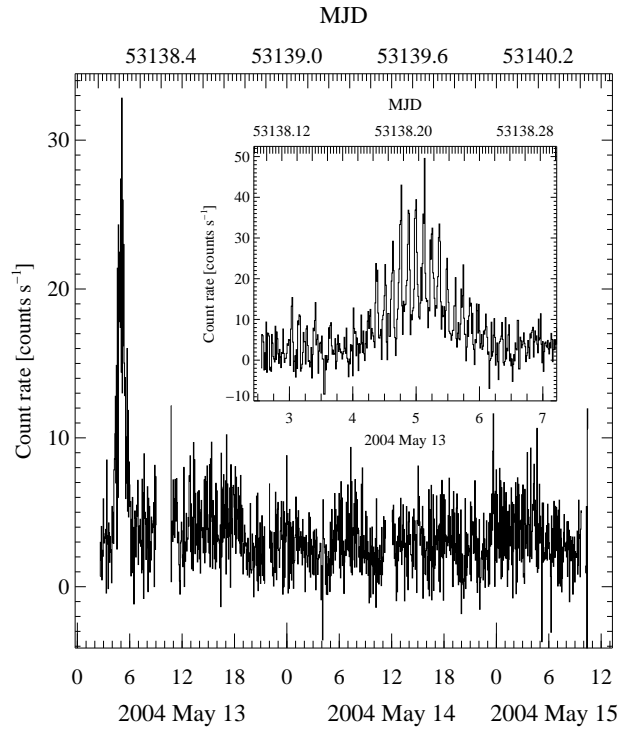


Figure 2. IBIS (ISGRI) 20–40 keV light curve of revolution 193 [from 9]. The bin time is 200 s. The inset shows a close up of the flare, the bin time in this case is 40 s. X-axis numbers are hours.

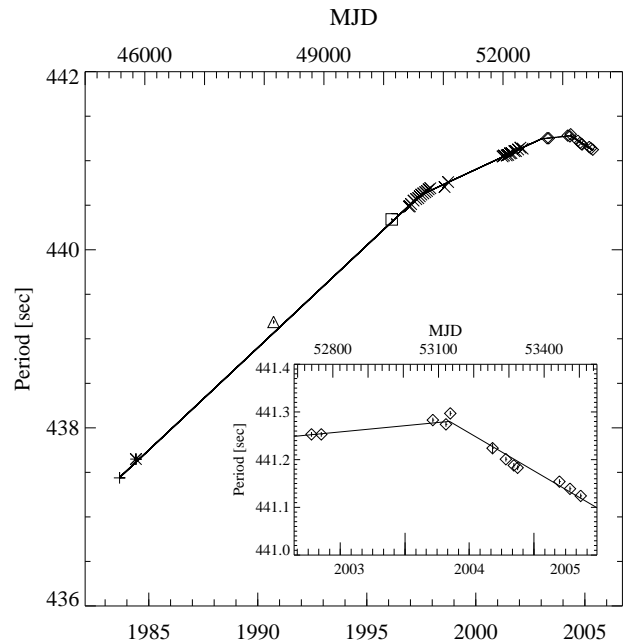


Figure 3. Evolution of the 4U 1907+09 pulse period over the last 20 years [as shown by 9]. Diamonds indicate the results obtained in this work, other symbols indicate data from [23, plus-signs], [5, asterixes], [25, triangles], [16, squares], and [1, 2, crosses]. Note the clear deviation from the long term trend leading to a complete spin reversal. The inset shows a closeup of the periods found by *INTEGRAL* [9].

the pulse period by first using epoch folding [22] to get a starting period and then performing pulse phasing to get a higher accuracy. Fig. 3 shows the long-time history of the period evolution based on all available data. Note that the recent periods obtained from *RXTE*-data [2] show a clear deviation from the historic spin down trend of  $\dot{P}_{\text{pulse}} = +0.225 \text{ s yr}^{-1}$  from [15]. The periods obtained by Fritz et al. [9] from *INTEGRAL*-data (shown as diamonds) not only confirm this change of the trend, but show a complete trend reversal from the historic long term spin down trend to a spin up trend from MJD 53131 onwards (see Fig. 3).

Using the derived periods, Fritz et al. [9] obtained pulse profiles for all revolutions (Fig. 4) by folding the light curves with the best respective periods. No change in the shape of the pulse profile is obvious, especially no change in the shape before, during, and after the reversal of  $\dot{P}$  can be seen.

## 2.2. Discussion

In the *INTEGRAL* data, a spin up phase of 4U 1907+09 is clearly detected after 20 years of spin down (Fig. 3) at a rate of  $\dot{P}_{\text{pulse}} = +0.225 \text{ s yr}^{-1}$ , with the available data being consistent with  $\ddot{P} = 0 \text{ s}^{-1}$ . In 2002 and 2003 first indications for a decrease in the magnitude of spin down were detected [2]. As shown in Sect. 2.1, the new *INTEGRAL* data show a torque reversal from  $\sim \text{MJD } 53131$  onwards, with the source now exhibiting a spin up with a rate of  $\dot{P}_{\text{pulse}} = -0.158 \text{ s yr}^{-1}$ . So far, the *INTEGRAL* results appear to be consistent with  $\ddot{P} = 0 \text{ s}^{-1}$  (the  $1\sigma$  upper limit for  $\ddot{P}$  during the spin up is  $-4 \cdot 10^{-5} \text{ s}^{-1} \text{ yr}^{-2}$ ).

The conventional interpretation of spin up in accreting X-ray pulsars with a strongly magnetized, disk-accreting neutron star is that the accretion disk is truncated by the magnetic field of the neutron star [see, e.g., 10, 11, 12, and references therein]. The transfer of angular momentum from the accreted matter onto the neutron star will lead to a torque onto the neutron star resulting in spin up. The general expectation of these models is that the Alfvén radius  $r_m$ , where the accretion flow couples to the magnetic field, is assumed to be close to the co-rotation radius,  $r_{\text{co}}$ .

This simple model, however, is unable to explain the long episodes of constant  $\dot{P}$ . For 4U 1907+09 the magnetospheric radius inferred from the cyclotron line measurements is  $r_m \sim 2400 \text{ km}$ , while  $r_{\text{co}} \sim 12000 \text{ km}$  [16]. Moving  $r_m$  out to  $r_{\text{co}}$  would require a magnetic field of  $\sim 10^{14} \text{ G}$  as for a magnetar, which is two orders of magnitude larger than the magnetic field deduced from the observed cyclotron lines.

Fritz et al. [9], however, then discuss that the a model presented recently by Perna et al. [28] is able to explain these observations. This model is based on the fact that X-ray pulsars are oblique rotators, i.e., the neutron star's magnetic field is tilted by an angle  $\chi$  with respect to the axis

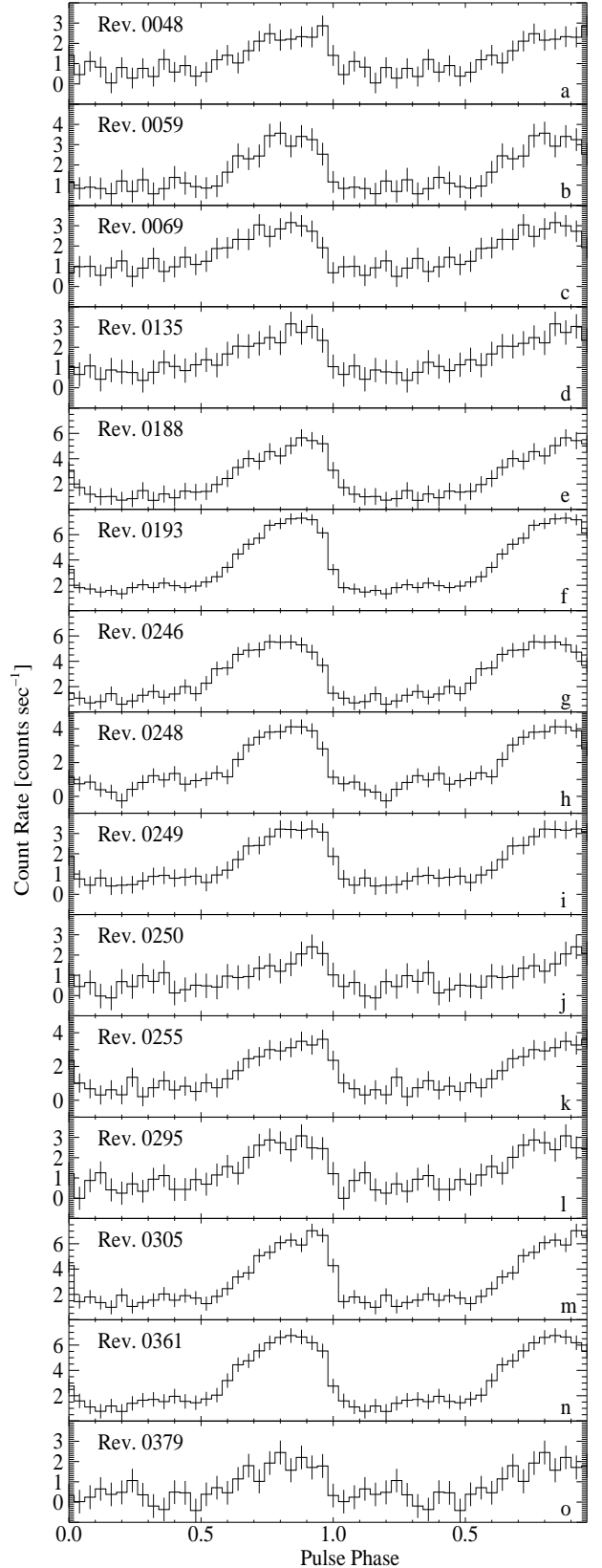


Figure 4. Pulse profiles for different revolutions in the 20–40 keV band [from 9]. Panels a–e show pulse profiles obtained during the period of spin down, and panels f–o show spin up pulse profiles.

of rotation of the neutron star. Assuming the accretion disk is situated in the neutron star's equatorial plane, for a ring of matter in the accretion disk, the magnetic field strength then depends on the azimuthal angle and thus the boundary of the magnetosphere is asymmetric. Such a configuration can lead to regions in the disk where the propeller effect is locally at work, while accretion from other regions is possible. This then results in a nonlinear dependence of the accretion luminosity from the  $\dot{M}$  through the outer parts of the disk. Perna et al. [28] point out that a nontrivial consequence is that for values of  $\chi$  greater than a critical value,  $\chi_{\text{crit}}$ , limit cycles are present, where cyclic torque reversal episodes are possible without a change in  $\dot{M}$ . For typical parameters,  $\chi_{\text{crit}}$  is between  $\sim 25^\circ$  and  $\sim 45^\circ$ . Perna et al. [28] and Fritz et al. [9] stress that the existence of the limit cycles depends only on  $\chi$  and on the pulsar's polar magnetic field,  $B$ , and no variation of external parameters is required to trigger torque reversals, while the torque reversal of 4U 1907+09 with no associated drop in luminosity and no change in the shape of the pulse profile is difficult to explain in conventional models.

### 3. V 0332+53

The recurrent X-ray transient V 0332+53 experienced an X-ray outburst from December 2004 to February 2005 [19, 29]. The outburst was predicted almost one year before the actual outburst [14] due to the optical brightening of the optical companion BQ Cam, a O8-O9e star.

The observation of this outburst of V 0332+53 by *RXTE* revealed the presence of three cyclotron lines [4, 19, 29]. The fundamental CRSF has an energy of 28 keV, and the first and second harmonics are at 50 keV and 71 keV, respectively. This corresponds to a magnetic field strength of  $2.7 \times 10^{12}$  G [19, 29]. The spectrum is otherwise described by a power law modified by a high-energy cut-off at higher energies.

#### 3.1. Fluxes

The light curve of V 0332+53 in ISGRI and JEM-X during the outburst is shown in Fig. 5. Mowlavi et al. [27] describe the decline phase by an exponential decay up to  $\text{MJD} \approx 53412$ , followed by a linear decrease. The exponential decay is less rapid at the ISGRI energies than at the JEM-X energies. From a simple estimation, the exponential decay time is about 30 days above 20 keV (solid curves in Fig. 5a) and about 20 days below 15 keV (solid curves in Fig. 5b). The exponential decay is also confirmed by the 2–12 keV light curve as observed by the All Sky Monitor (ASM) on board of *RXTE* (see Fig. 5b).

Reig et al. [30] discovered a very interesting behavior of the color-color diagram over the outburst (see Fig. 6). They derived background-subtracted light curves corresponding to the energy ranges  $c_1 = 4 - 7.5$  keV,  $c_2 =$

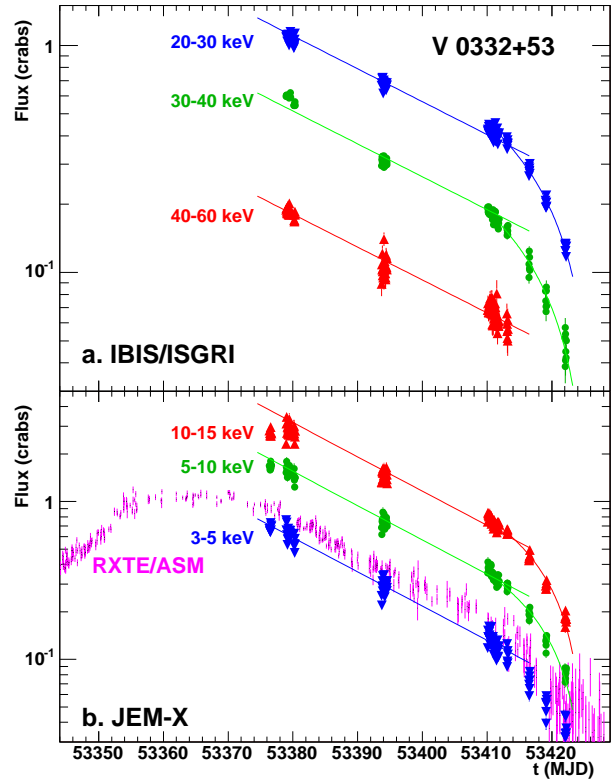


Figure 5. **a** Light curve of V 0332+53 over the decay of the outburst in different energy bands in Crab units [as shown by 27]. The solid curves are fits to the exponential (from  $\text{MJD}=53376$  to  $53412$  with  $\tau=30$  days) and linear (from  $\text{MJD}=53412$  to  $53422$ ) **b** Same as **a**, but for JEM-X fluxes and with an exponential decay of  $\tau=20$  days. The 2–12 keV *RXTE*/ASM light curve is also shown, using a normalization factor of 77 cps for 1 Crab.

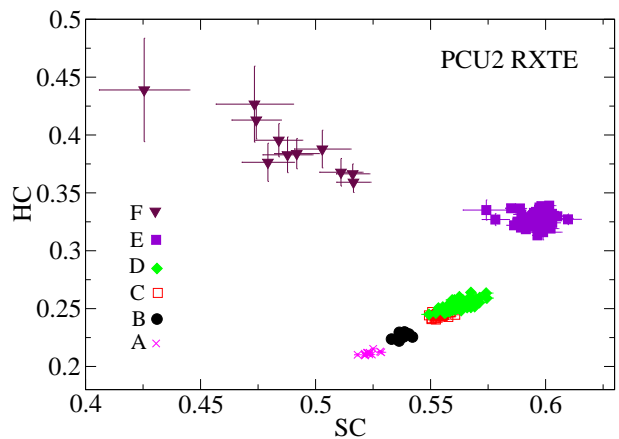


Figure 6. Color-Color Diagram of the outburst of V 0332+53 [from 30] using *RXTE*-data. The X-ray colors are defined as soft color  $SC=7.5-10$  keV/4–7.5 keV and hard color  $HC=15-30$  keV/10–15 keV.

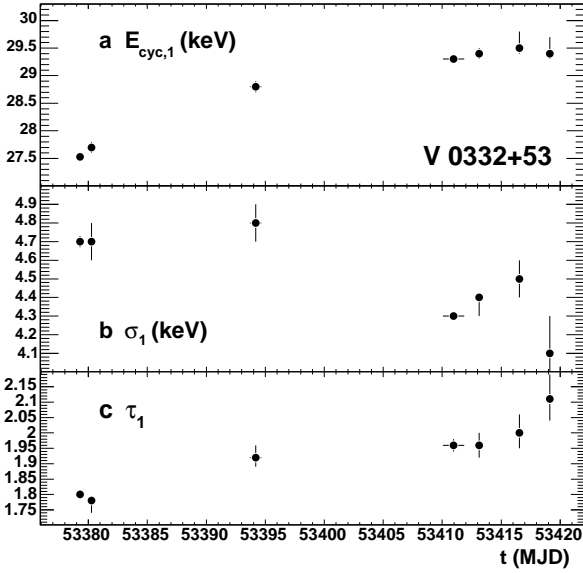


Figure 7. Evolution of the parameters of the fundamental cyclotron line [from 27]. **a** line energy, **b** width, and **c** depth. The vertical bars represent 90% uncertainty, while the horizontal bars indicate the duration of each observation.

7.5 – 10 keV,  $c_3 = 10 - 15$  keV and  $c_4 = 15 - 30$  keV and then defined the soft color (SC) as the ratio  $c_2/c_1$  and the hard color (HC) as the ratio between  $c_4/c_3$ .

These authors observed that the source was in a soft state during the peak of the outburst and as the count rate decreased the source moved up and right in the color color diagram, i.e. it became harder. At the end of the outburst (regions E and F) the source moved again to the left, i.e., lower values of SC, while HC remained mostly constant. Therefore two spectral states or branches can be distinguished: a soft state when the source is bright and a hard state when the source gets dimmer.

The pattern in the color color diagram of V 0332+53 resembles that of low mass X-ray binary Z source [see e.g 34]. In this picture, the soft branch would correspond to the normal branch and the hard branch to the horizontal branch in a Z source, however, as Reig et al. [30] point out, the flaring branch observed in Z source is missing in V 0332+53. During the decline of the outburst, the source moves without jumps through the Z shape in the color color diagram, taking about 80 days from the softest to hardest point [30].

### 3.2. Spectrum

The spectra of accreting X-ray pulsars are a superposition of contributions from the hotspots at both magnetic poles and the lower parts of the accretion columns. Since no self consistent model is available, various empirical models have to be used [18]

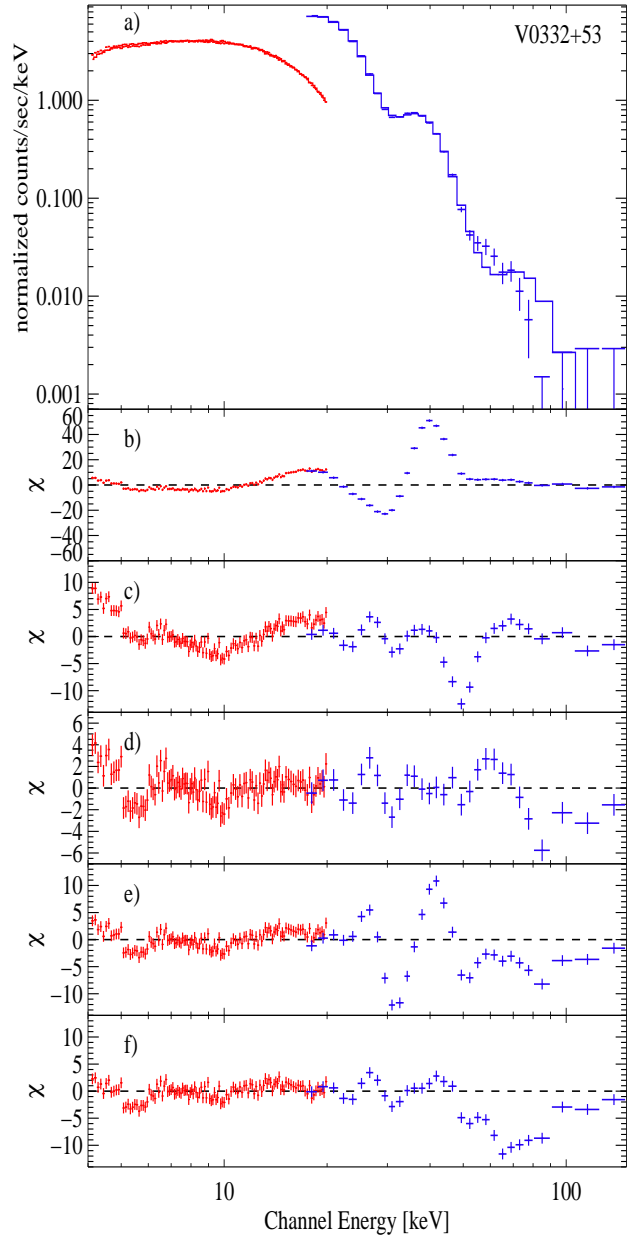


Figure 8. **a** Spectrum and folded model for JEM-X (left) and ISGRI (right) using data of revolution 284 [from 27]; **b** residuals of the model with  $\Gamma = -0.41$  and  $E_{\text{fold}} = 7.4$  keV, and without any cyclotron line modeled; **c** one Gaussian is included at 29.3 keV; **d** a second Gaussian is added at 51 keV to model the first harmonic; **e** as before, but with the energy of the first line fixed at 27.5 keV, the value found in revolution 273; **f** same as **d**, but with  $\Gamma$  fixed to the value of  $-0.17$  found in revolution 273. The strong residuals in the two bottom panels show that the parameters of the fundamental cyclotron line do indeed change.

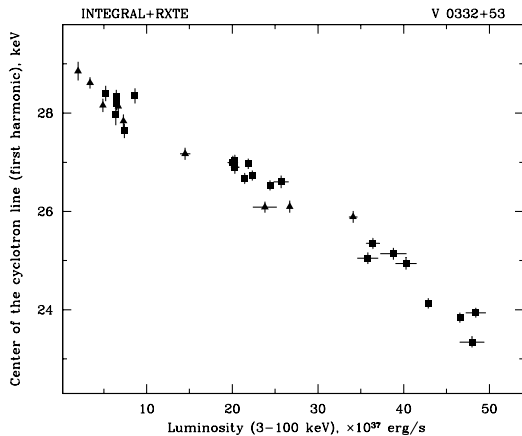


Figure 9. Dependence of the energy of the energy of the fundamental cyclotron line of V0332+53 [from 33]. Triangles represent results from INTEGRAL, and squares from RXTE.

Mowlavi et al. [27] use the simple “cutoffpl” model to fit the combined ISGRI and JEM-X data, to which two cyclotron lines with a Gaussian optical depth profile [3] have been added. A multiplicative constant is applied to allow for the different normalizations of the two instruments. Furthermore a systematic error of 2% is applied to account for the uncertainties in the response matrices of JEM-X and ISGRI. No photoelectric absorption is required at low energies, compatible with the fact that the JEM-X data are analyzed only above 4 keV. The same model is used for all observations to keep consistency between the parameters from one observation to the next.

The cyclotron line parameters for the fundamental line [27] are displayed in Fig. 7 as a function of time. The spectrum with the fits and the residuals for a model with no, one, two, and three cyclotron lines using the data of revolution 284 is shown in Fig. 8. The energy of the fundamental cyclotron line increases by 7% from the first to the last *INTEGRAL* observations, and the depth of the line increases by 16% while at the same time the width decreases by 12%. These changes are significant; according to Mowlavi et al. [27], the attempt to fit the spectrum in revolution 284 with a line at 27.5 keV results in strong residuals around the line (Fig. 8e), but also variations of continuum can be ruled out to explain the changes in the line parameters (Fig. 8f).

Tsygankov et al. [33] then went one step further and instead plotting the energy of the fundamental cyclotron line versus time, these authors show the dependence of the cyclotron energy on the luminosity of the source, thus combining Figs. 7 and 5 into Fig. 9. A linear fit to this

dependence results in the following relation:

$$E_{\text{cyc},1} = -0.10L_{37} + 28.97\text{keV},$$

where  $L_{37}$  is the luminosity in units of  $10^{37}\text{erg s}^{-1}$ . Assuming that for low luminosities the emission comes practically from the neutron star surface, Tsygankov et al. [33] estimate the magnetic field on the surface of the neutron star for canonical values for the radius and the mass of the neutron star to  $B = 3.0 \cdot 10^{12}\text{G}$ .

### 3.3. Discussion

V 0332+53 is a highly magnetized pulsar with a magnetic field of about  $3.0 \times 10^{12}\text{G}$  [19, 29, 33], as derived from the energy of the fundamental cyclotron line. The X-ray outbursts from this system are observed with a time recurrence of about 10 years. They are believed to be triggered by a massive mass ejection from the optical companion star, resulting in the optical brightening of the system in 2004 [14]. The ejected mass feeds an accretion disk around the pulsar, from which it is funneled by the magnetic field towards the polar caps and falls on the surface of the neutron star.

The analysis of the 2005 outburst provides new insights towards a better understanding of V 0332+53 and similar transient sources within this basic picture. The X-ray light curve (Sect. 3.1) displays a characteristic exponential decay with a time scale of 20 to 30 days, followed by a linear decrease. This remarkable change occurs approximately at the same moment when the trend in the color color diagram changes. This may provide some information on the accretion and especially the geometry.

As discussed by Mowlavi et al. [27], an exponential decay of the flux is observed also in dwarf novae and in soft X-ray transients on time scales from a few days for the former to several weeks for the latter [21, 32]. King & Ritter [17] show how illuminated disks in low-mass X-ray binary stars can produce such an exponential decay on the time scales observed for the soft X-ray transients. Subsequently, numerical calculations by Dubus et al. [8] showed, that indeed irradiated accretion disks produce an exponential decay of the X-ray luminosity.

As Mowlavi et al. [27] point out, it is tempting to make the parallel with the results observed in V 0332+53. The exponentially decreasing flux followed by a linear decrease is very similar to what is observed in disk-illuminated systems. Such a behavior as observed by Mowlavi et al. [27] has never before been observed in a high mass accreting X-ray binary pulsar system. The X-ray flux is proportional to the mass accretion rate, and therefore the accretion rate would then also be proportional to the mass of the disk. An unknown change in the disk would then trigger the switch to the linear decay phase. Furthermore, Mowlavi et al. [27] suggest that the two different decay times observed in V 0332+53 are due to the presence of at least two regions contributing to the X-ray continuum: one time scale governs the

rate of mass flow onto the neutron star through the disk, leading to the exponential decay followed by a linear decrease (see above); another time scale governs the spectral changes of the emission that may come from different heights within the accretion column [27].

The X-ray spectrum (Sect. 3.2) is well fitted by a cutoff power law modified by two cyclotron lines. The energy of the fundamental cyclotron line is shown to increase by 20% from the peak of the outburst as measured by *RXTE* until the end of the outburst. At the same time it became narrower and deeper. This information would provide some insight into the resonance scattering region near the polar caps. The evolution of cyclotron line parameters with time has already been reported in the literature for several binary systems [25]. These authors attribute the change of the line energy to a change of the height of the scattering region above the neutron star, resulting in a height change  $\sim 300$  m for V 0332+53. Kreykenbohm et al. [20] report a variation of the cyclotron energy of GX 301-2 with the pulse phase of the pulsar, and attribute the change to different viewing angles of the accretion column where the line originates.

For V 0332+53 Mowlavi et al. [27] interpret the increase of the energy as a variation of the scattering region characteristics. They assume that the region where the cyclotron resonance scattering takes place is extended. The region would then cover a range of magnetic field strengths resulting in a superposition of several narrow cyclotron lines, each originating at a specific height and therefore in a specific magnetic field strength, thus giving rise to a broad line. As the accretion rate and hence the flux decreases with time, the cyclotron resonance region shrinks and moves closer to the neutron star. At the end of the outburst only the region closest to the neutron star surface, where the magnetic field is strongest, would contribute to the formation of cyclotron lines. The resulting lines can therefore be expected to be observed at higher energies and being much narrower as is indeed observed in V 0332+53. Mowlavi et al. [27] estimate the total movement of the cyclotron line formation region to be of the order of 500 m, similar to 4U 0115+63 where a change of  $\sim 1$  km was observed [26].

## ACKNOWLEDGMENTS

We acknowledge the support of the Deutsches Zentrum für Luft- und Raumfahrt under grant numbers 50OR0302, 50OG9601, and 50OG0501, and by National Aeronautics and Space Administration grant INTEG04-0000-0010.

## REFERENCES

- [1] Baykal, A., Ç. İnamAlpar, M. A., et al. 2001, *MNRAS*, 327, 1269–1272
- [2] Baykal, A., İnam, S. Ç., Beklen, E. 2006, *MNRAS*, 369, 1760–1764
- [3] Coburn, W., Heindl, W. A., Rothschild, R. E., et al. 2002, *ApJ*, 580, 394–412
- [4] Coburn, W., Kretschmar, P., Kreykenbohm, I., et al. 2005, *ATel*, 381
- [5] Cook, M. C., Page, C. G. 1987, *MNRAS*, 225, 381–392
- [6] Cox, N. L. J., Kaper, L., Foing, B. H., Ehrenfreund, P. 2005, *A&A*, 438, 187–199
- [7] Cusumano, G., Di Salvo, T., Burderi, L., et al. 1998, *A&A*, 338, L79–L82
- [8] Dubus, G., Lasota, J.-P., Hameury, J.-M., Charles, P. 1999, *MNRAS*, 303, 139–147
- [9] Fritz, S., Kreykenbohm, I., Wilms, J., et al. 2006, *A&A*, 458, 885–893
- [10] Ghosh, P., Lamb, F. K. 1978, *ApJL*, 223, L83–L87
- [11] Ghosh, P., Lamb, F. K. 1979, *ApJ*, 232, 259–276
- [12] Ghosh, P., Lamb, F. K. 1979, *ApJ*, 234, 296–316
- [13] Giacconi, R., Kellogg, E., Gorenstein, P., et al. 1971, *ApJL*, 165, L27–L35
- [14] Goranskij, V., Barsukova, E. 2004, *ATel*, 245, 1
- [15] in ’t Zand, J. J. M., Strohmayer, T. E., Baykal, A. 1997, *ApJ*, 479, L47–L50
- [16] in ’t Zand, J. J. M., Baykal, A., Strohmayer, T. E. 1998, *ApJ*, 496, 386–394
- [17] King, A. R., Ritter, H. 1998, *MNRAS*, 293, L42–L48
- [18] Kreykenbohm, I., Kretschmar, P., Wilms, J., et al. 1999, *A&A*, 341, 141–150
- [19] Kreykenbohm, I., Mowlavi, N., Produit, N., et al. 2005, *A&A*, 433, L45–L48
- [20] Kreykenbohm, I., Wilms, J., Coburn, W., et al. 2004, *A&A*, 427, 975–986
- [21] Lasota, J.-P., Narayan, R., Yi, I. 1996, *A&A*, 314, 813–820
- [22] Leahy, D. A., Darbo, W., Elsner, R. F., et al. 1983, *ApJ*, 266, 160–170
- [23] Makishima, K., Kawai, N., Koyama, K., et al. 1984, *PASJ*, 36, 679–689
- [24] Makishima, K., Mihara, T., Nagase, F., Murakami, T. 1992, in Tanaka, Y., Koyama, K., *Frontiers of X-Ray Astronomy, Proc. XXVIII Yamada Conf.*, Frontiers Science Series, 2, 23–32
- [25] Mihara, T., PhD thesis, RIKEN, Tokyo, 1995
- [26] Mihara, T., Makishima, K., Nagase, F. 1998, in *All Sky Monitor Survey Conference*, 135–140 RIKEN
- [27] Mowlavi, N., Kreykenbohm, I., Shaw, S. E., et al. 2006, *A&A*, 451, 187–194
- [28] Perna, R., Bozzo, E., Stella, L. 2006, *ApJ*, 639, 363–376
- [29] Pottschmidt, K., Kreykenbohm, I., Wilms, J., et al. 2005, *ApJ*, 634, L97–L100
- [30] Reig, P., Martínez-Núñez, S., Reglero, V. 2006, *A&A*, 449, 703–710

- [31] Roberts, M. S. E., Michelson, P. F., Leahy, D. A., et al. 2001, *ApJ*, 555, 967–977
- [32] Tanaka, Y., Shibazaki, N. 1996, *ARA&A*, 34, 607–644
- [33] Tsygankov, S. S., Lutovinov, A. A., Churazov, E. M., Sunyaev, R. A. 2006, *MNRAS*, 371, 19–28
- [34] van der Klis, M. in Lewin, W. H. G., van Paradijs, J., van den Heuvel, E. P. J., *X-ray binaries*, Cambridge University Press, Cambridge, 1995